Substrate-Dependent Inhibition Kinetics of an Active Site-Directed Inhibitor of ADAMTS-4 (Aggrecanase 1)

Arthur J. Wittwer,* Robert L. Hills, Robert H. Keith, Grace E. Munie, Elizabeth C. Arner, Charles P. Anglin, Anne-Marie Malfait, and Micky D. Tortorella

Pfizer Global Research and Development, 700 Chesterfield Parkway, Chesterfield, Missouri 63017

Received January 12, 2007; Revised Manuscript Received March 23, 2007

ABSTRACT: ADAMTS-4 (aggrecanase-1) is implicated in the breakdown of articular cartilage and is an attractive target for therapeutic intervention in arthritis. Cleavage of the native substrate, aggrecan, occurs through exosite interactions and peptide sequence recognition. Although expected to be competitive with aggrecan, the hydroxamic acid, SC81956, demonstrated noncompetitive inhibition kinetics with a K_i of 23 nM. The IC_{50} of SC81956 did not change when aggrecan was varied from 12.8 to 200 nM (0.2−3.3 times the apparent aggrecan K_m of 61 nM) but was shifted as expected for a competitive inhibitor when increasing levels of a low molecular weight peptide substrate were added to a fluorogenic peptide assay system. These observations are consistent with a model for aggrecan cleavage where substrate initially binds at an exosite, followed by binding of the appropriate peptide sequence at the active site. A peptide-competitive inhibitor could bind both free enzyme and initial substrate−enzyme exosite complex but would be excluded by the final Michaelis complex. Noncompetitive appearing kinetics for such inhibitors is predicted as long as the equilibrium between the two forms of enzyme−substrate complex significantly favors the initial exosite complex. In support, hydrolysis of a low molecular weight peptide substrate and its inhibition by SC81956 were unaffected by aggrecan concentrations substantially above the K_m. These observations suggest that the apparent K_m for aggrecan cleavage predominately reflects the exosite interaction. Consequently, the efficacy of active-site inhibitors of ADAMTS-4 will not be limited by competition with native substrate as predicted from the K_m determined by traditional kinetic models.

ADAMTS-4, also referred to as aggrecanase-1, is a member of the ADAMTS[1] (a disintegrin and metalloproteinase with thrombospondin motifs) protein family (*1*). Members of the family share several distinct protein modules, including a propeptide region, a metalloproteinase domain, containing the canonical HExxHxxxxxH zinc metalloproteinase motif, a disintegrin-like domain, and a thrombospondin type 1 (TS) motif. Individual members of this family differ in the number of C-terminal TS motifs, and some have unique C-terminal domains (*2*). ADAMTS-4 and ADAMTS-5 cleave aggrecan, a proteoglycan and one of the major macromolecules of articular cartilage, efficiently and with high specificity. ADAMTS-4 prefers glutamic acid at P1 and cleaves the aggrecan core protein at Glu^{373}, Glu^{1545}, Glu^{1714}, Glu^{1819}, and Glu^{1919} (human sequence) (*3*). The cleavage of aggrecan suggests a key role of this enzyme in arthritis and makes ADAMTS-4 and ADAMTS-5 attractive targets for therapeutic intervention.

Aggrecan is a glycoprotein that consists of a protein backbone of 210−250 kDa to which both chondroitin sulfate (CS) and keratan sulfate (KS) chains are attached (*4*). These sulfated glycosaminoglycan (GAG) chains are attached to the central portion of the core protein, CS chains (100−150 per monomer), being located in the C-terminus, whereas KS (30−60 per monomer) is preferentially located toward the N-terminus. Individual aggrecan monomers, up to 100, interact with hyaluronic acid to form an aggregate of very high molecular weight. This interaction involves a globular domain at the N-terminus, termed G1 or the hyaluronic acid binding region. The interaction is stabilized by a short protein called link protein, which interacts with both hyaluronic acid and G1. A further globular domain close to G1 on the aggrecan core protein is termed G2. Although it is not involved in the binding with either link protein or hyaluronic acid, it shares considerable sequence homology with G1. A third globular domain, G3, is located at the C-terminus and has three structural domains: an epidermal growth factor repeat, a lectin-like sequence, and a region homologous to the complement regulatory protein motif.

The TS motif located within the C-terminus of ADAMTS-4 is critical for aggrecan binding and cleavage, representing a potential extended macromolecular interaction site or exosite. ADAMTS-4 binds aggrecan through interaction of its TS motif with the sulfated GAG side chains of aggrecan with a K_d of ∼11 nM, referring to the aggrecan concentration required for half-maximal binding (*5*) (Figure 1). Removal of these side chains from aggrecan results in a significant decrease of ADAMTS-4 binding and cleavage. In addition, peptides corresponding to regions of the TS motif block both binding of ADAMTS-4 and subsequent cleavage

* To whom correspondence should be addressed. Phone: 1-636-247-7342. Fax: 1-636-247-7223. E-mail: arthur.j.wittwer@pfizer.com.

[1] Abbreviations: ADAMTS, a disintegrin and metalloproteinase with thrombospondin motifs; CS, chondroitin sulfate; KS, keratan sulfate; GAG, glycosaminoglycan; TS, thrombospondin type 1; DMSO, dimethylsulfoxide; IL-1, interleukin-1.

10.1021/bi7000642 CCC: $37.00
Published on Web 05/08/2007

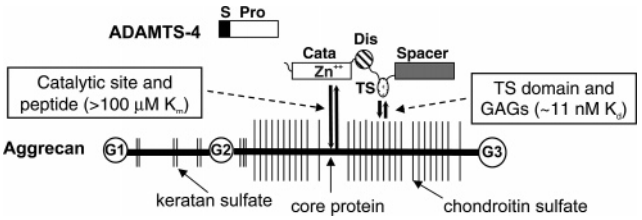

FIGURE 1: Schematic diagram illustrating the binding and cleavage of aggrecan by ADAMTS-4. G1, globular domain 1; G2, globular domain 2; G3, globular domain 3; S, signal sequence; Pro, propeptide domain; Cata, catalytic domain; DIS, disintegrin domain; TS, thrombospondin domain.

of native aggrecan. For example, the peptide ^{521}GGWGP-WGPWGD^{531}, corresponding to the sequence implicated in the interaction of the TS motif with sulfated GAG chains, was effective in blocking cleavage of aggrecan with an IC_{50} of 17 μM. Extension of the peptide to include the sequence ^{532}CSRTCG^{537}, representing a putative CD36-binding region in thrombospondin, resulted in a peptide that was more potent in inhibiting aggrecan cleavage ($IC_{50} = 3$ μM). Finally, a recombinant truncated form of ADAMTS-4 including amino acids 213−431 that lacks the C-terminal domains (including the TS motif) does not bind or cleave aggrecan, consistent with the fact that the C-terminal region of the enzyme is important for substrate recognition (*5*).

To date, only small molecule active site directed inhibitors that coordinate the essential Zn^{++} of ADAMTS-4 have been described (*6*, *7*). In these studies, hydroxamate-based inhibitors with nanomolar potency were reported. Considering their mechanism of inhibition, these hydroxamate-based inhibitors would be expected to be competitive with substrate. However, we are unaware of any studies examining the inhibition kinetics of aggrecan cleavage by aggrecanases. Because of the difficulties inherent in macromolecular substrate assays, several peptide substrates of ADAMTS-4 have been developed, which bracket the Glu^{373} cleavage site in aggrecan. These include a 41-residue peptide employed in an ELISA based assay, NH2-QTVTWPDMELPLPRNITEGE*ARG-SVILTVKPIFEVSPSPLK-biotin (* demarcates the scissile bond) (*8*), and a 13-residue peptide substrate used in a fluorogenic assay, Abz-TEGE*ARGSVI-Dap(Dnp)-KK (*9*). To our knowledge there has also been no report of the inhibition kinetics of aggrecanase employing such small peptide substrates.

It is important to consider that artificial peptide substrates may not interact with potential exosites in the same manner as the native substrate. In the case of ADAMTS-4, the interaction of the TS motif with the CS and KS chains of aggrecan is eliminated. Thus, if the exosite interaction of the TS motif mediates binding, this raises the question of whether or not competitive inhibitors of ADAMTS-4 will demonstrate classical competitive behavior with respect to the native substrate aggrecan. Indeed, in the case of several coagulation proteases, where exosites importantly figure into substrate recognition and specificity, inhibitors competitive with small peptide substrates appear noncompetitive with the native pro-enzyme substrates (*10*).

The goals of this study were to (1) compare the inhibition kinetics of a hydroxamate-based inhibitor of ADAMTS-4 using a small peptide substrate versus the native substrate, aggrecan; (2) define the mode of inhibition of the ADAMTS-4 inhibitor with both substrates; and (3) describe a kinetic model that will explain the observed inhibition kinetics.

MATERIALS AND METHODS

Aggrecanase Inhibition Assay. Inhibition of ADAMTS-4 or ADAMTS-5 cleavage at the Glu^{373}-Ala^{374} site of aggrecan was measured as follows. Full-length recombinant ADAMTS-4 and -5 were expressed in SF9 cells and purified as previously described (*1*). Reaction mixtures of 100 μL final volume in 96-well polypropylene plates contained purified bovine aggrecan (*3*), 0.2 nM ADAMTS-4 or ADAMTS-5, and inhibitor or 1.0% dimethylsulfoxide (DMSO) vehicle control in 50 mM Tris buffer at pH 7.5, containing 100 mM NaCl and 5 mM $CaCl_2$. The concentration of aggrecan was 125 nM for IC_{50} determinations or ranged from 5.12 to 200 nM for ADAMTS-4 kinetic analyses. After a 6-h incubation at 37 °C, the reaction was stopped with the addition of 10 μL 0.5 M EDTA, and 75 μL was transferred to a 96-well PVDF membrane plate (Millipore, Billerica, MA) containing 75 μL of 20 mM carbonate−bicarbonate buffer at pH 9.6 (Sigma, St. Louis, MO). Prior to the addition of the carbonate−bicarbonate buffer, the PVDF plates had been conditioned for 5 min with 100 μL 70% ethanol in water and washed two times with 200 μL water. Plate washing was facilitated by using a Tecan Columbus Plus plate washer (Research Triangle Park, NC) modified with the addition of a vacuum manifold by Flush Tec (Cathedral City, CA). The samples were allowed to bind to the PVDF plates overnight at room temperature, washed twice with 200 μL Tris-buffered Saline (TBS) (Bio-Rad Laboratories product #170-6435), and incubated for 3 h at 37 °C with 0.1 units/mL chondroitinase ABC, 0.1 units/mL keratanase, and 0.01 units/mL keratanase II (Associates of Cape Cod, East Falmouth, MA), in 100 μL of 50 mM Tris, 100 mM sodium acetate buffer at pH 6.5, containing 1% BSA. The plates were washed twice with 200 μL TBS and incubated for 1 h at room temperature with 2 μg/mL BC-3 antibody and 1 μg/mL goat anti-mouse IgG conjugated to alkaline phosphatase (Promega, Madison, WI) in 100 μL TBS containing 1% BSA buffer. The monoclonal neoepitope antibody BC-3 recognizes the new N-terminus ^{374}ARGS on aggrecan fragments produced by cleavage at the Glu^{373}−Ala^{374} bond and was licensed from Dr B. Caterson (University of Wales, Cardiff, UK) (*11*)) The plate was then washed three times with 200 μL TBS, and alkaline phosphatase was detected by the addition of 100 μL of *p*-nitrophenyl phosphate substrate (Sigma-Aldrich Co., product P7998). After 20 min of incubation at room temperature, the reaction was stopped with the addition of 100 μL of 0.5 M EDTA, and 150 μL was transferred to a flat-bottomed 96-well transparent plate (Corning, Corning, NY) for reading absorbance at 405 nm.

Bovine Nasal Cartilage Assay. Cartilage was dissected from the nasal septa of young cows obtained from Covance Research Products (Denver, PA). Cartilage was allowed to equilibrate for 3 days in Dulbecco's Modified Eagle's Medium (DMEM) supplemented with 10% fetal calf serum (FCS), penicillin (100 U/mL) and streptomycin (100 μg/mL), all purchased from Invitrogen (Carlsbad, CA). Subsequently, cartilage was cut into 3 × 3 mm explants, weighing approximately 10−20 mg each, and incubated in 96-well plates for 48 h with control medium (serum-free DMEM),

medium containing interleukin-1β (IL-1β) (10 ng/mL), or medium containing IL-1β (10 ng/mL) plus SC81956 at 3−3000 nM. Eight explants were used for each treatment group. At the end of the culture period, supernatants were collected and frozen at −20 °C for further assays. Glycosaminoglycan content of the supernatants was determined using the dimethylmethylene blue assay, as described by Farndale et al. (*12*). Shark chondroitin sulfate was used as a standard, and results were expressed as μg of GAG per mg of wet weight cartilage. The release of aggrecan fragments containing the ^{374}ARGS neoepitope was determined using PVDF membrane plates and the BC-3 antibody as described above for the aggrecanase inhibition assay, except that 20 μL of supernatant was used.

Peptide Substrate Assay. Peptide-B06 is a fluorescently labeled and quenched substrate of ADAMTS-4 with the sequence NH_2-K(6-(fluorescein-5-carboxamido)-hexanoic acid)-DVQEFRGVTAVIR-C(QSY9)-KGK-COOH, where C(QSY9) is the reaction product of the fluorogenic molecule QSY9 (Invitrogen Corporation) with the -SH group of the cysteine residue. ADAMTS-4 cleaves the Glu−Phe bond of Peptide-B06, accompanied by an increase in fluorescence at 519 nm upon excitation at 495 nm (*13*). Reactions were initiated by adding ADAMTS-4 (0.4 nM final) to 100 μL of a 1 μM solution of Peptide-B06 containing 20 mM Tris-HCl, 150 mM NaCl, 10 mM CaCl, and 0.01% Brij-35 at pH 7.5 and 37 °C, after which the rate of fluorescence increase was calculated by linear regression. The effect of purified bovine aggrecan on activity was determined by including it in the reaction mixtures at concentrations ranging from 0.01 to 5 μM. When the effect of aggrecan on the potency of SC81956 was determined, ADAMTS-4 was incubated with 0.05, 0.1, 0.5, or 1 μM aggrecan for 30 min at 37 °C. The reaction was initiated by adding Peptide-B06 (1 μM, final) premixed with various dilutions of SC-81956 (0.046−10 μM) or 1% final DMSO vehicle control.

Initial Rate Equation for Inhibition of Aggrecanase-Mediated Aggrecan Cleavage. A rate equation for the rapid equilibrium model described in Scheme 1 was derived from the relationships, $K_{S*} = [ES]/[ES^*]$, $K_S = [E][S]/[ES]$, $K_i = [E][I]/[EI]$, $\alpha K_i = [ES][I]/[ESI]$, $v = k_p[ES^*]$, and $[E]_t = [E]+[ES]+[ES^*]+[EI]$, by the established procedure (*14*). The expression is given as eq 1 below.

$$v = k_p[E]_t[S]/(K_S K_{S*}(1 + [I]/K_i) + [S](1 + K_{S*}(1 + [I]/\alpha K_i))) \quad (1)$$

In the simplest case, $\alpha = 1$, meaning that neither initial aggrecan binding to form the ES complex nor inhibitor binding change the binding affinity of the other to the enzyme. An identical model and rate equation were first proposed by Krishnaswamy and co-workers to explain the inhibition of prothrombinase (*15*). For consistency, the same symbols used by these authors are used here to denote the enzyme−substrate complex associated only at the exosite (ES), the enzyme−substrate complex associated at both the exosite and active site (ES*), and the dissociation constant for ES* (K_{S*}).

Demonstration that SC81956 and Peptide-A08 Are Mutually Exclusive Inhibitors of ADAMTS-4. Because of the low solubility of Peptide-B06, a more soluble peptide, Peptide-A08 (NH2-QEYKAHHSYKLMS-COOH), was employed for competition assays with SC81956. Peptide-A08 was shown to be an efficiently cleaved substrate of ADAMTS-4, with cleavage taking place between the E and Y residues (*13*). As an alternative substrate, it showed an apparent IC_{50} of 26 μM in the assay using Peptide-B06. Reaction mixtures containing Peptide-B06 at 1 μM, Peptide-A08 at 0, 25, 50, and 100 μM, and SC-81956 at 0, 0.0137, 0.0412, 0.123, 0.370, 1.11, 3.33, and 10 μM were incubated for 15 min at 37 °C. Reactions were initiated by the addition of the ADAMTS-4 enzyme at a final concentration of 0.4 nM and initial rates obtained as described above for the peptide substrate assay. Rates were analyzed as a function of SC81956 concentration to determine IC_{50} values at each concentration of Peptide-A08.

Scheme 1: Simplified Kinetic Model of Aggrecanase-Mediated Cleavage of Aggrecan and Inhibition by an Active Site Directed Inhibitor[a]

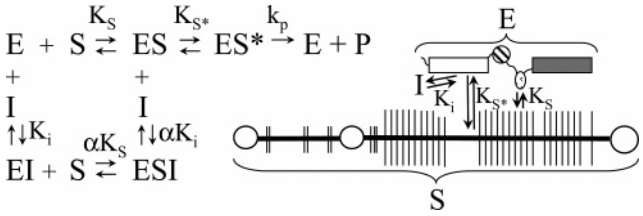

[a] S and E indicate substrate (aggrecan) and enzyme (aggrecanase), respectively, as detailed in Figure 1. I represents a low molecular weight aggrecanase inhibitor that competes with peptide substrates. K_i is the inhibitor dissociation constant, K_S is the dissociation constant of the enzyme−substrate complex bound only at the exosite. K_{S*} is the dissociation constant of the enzyme−substrate complex bound at both exosite and active site to yield the enzyme substrate complex bound only at the exosite. ES represents the enzyme−substrate complex bound only at the exosite; ES* represents the enzyme−substrate complex bound at both exosite and active site; EI represents the enzyme−inhibitor complex; ESI represents the ES−inhibitor complex; P represents reaction product; k_p is the rate constant for the formation of P from ES*; αK_S is the dissociation constant of the ESI complex to form EI and S; and αK_i is the dissociation constant of the ESI complex to form ES and I.

The ability of SC81956 and Peptide-A08 to act in a mutually exclusive fashion in their inhibitory effects was assessed by using the equation given by Copeland (*16*), modified to include a term for background activity in the absence of enzyme and SC81956, and allowing for an effect on this background by different levels of Peptide-A08.

$$v_{ij} = bkg_j + v_0/(1 + [I]/K_i + [J]/K_j + [I][J]/\alpha K_i K_j) \quad (2)$$

In eq 2, v_{ij} is the initial velocity in the presence of inhibitors I (SC81956) and J (Peptide-A08), bkg_j is the background activity at different levels of inhibitor J, v_0 is the uninhibited initial velocity, K_i and K_j are the inhibitor dissociation constants, and α is an interaction term describing the effect of one inhibitor on the inhibitory effect of the other. If α is infinite, this effect is mutually exclusive, suggesting competition between the two inhibitors (*16*). Fitting the data to this equation gave $K_i = 16.6$ nM, $K_j = 26.2$ μM, and an extremely large value for α (~1E17), suggesting a mutually exclusive interaction.

Data Fitting and Analysis. Nonlinear curve fitting was performed using the software program GraFit (Erithacus Software Ltd., Horley, UK) with appropriate modifications to the equations supplied. For fitting dose−response data

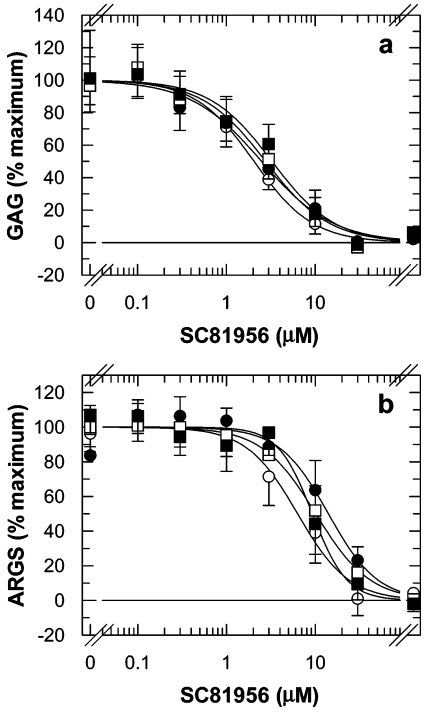

FIGURE 2: Potency of SC81956 is significantly decreased in a bovine nasal cartilage assay. Bovine nasal cartilage was stimulated with IL-1 (10 ng/mL) in the presence or absence of SC81956 at various concentrations ranging from 3 to 3000 nM. Following incubation, the release of GAG (a) and the release of ^{374}ARGS-containing aggrecan fragments (b) was monitored as described in Materials and Methods. Four separate dose−response curves are shown representing four different bovine tissues. The curves show the fits used for IC_{50} determinations. Points are the mean of 5−8 determinations, and error bars indicate the standard error of the mean. Points to the extreme right in each graph are from control cartilage that was not stimulated with IL-1.

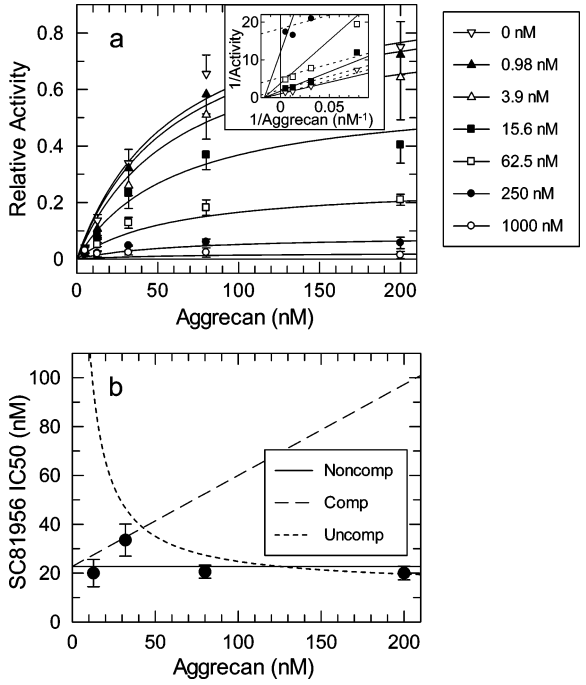

FIGURE 3: SC81956 does not demonstrate competitive inhibition of ADAMTS-4 with respect to aggrecan. (a) Aggrecanase inhibition assay results were obtained using the range of aggrecan and SC81956 concentrations as indicated. Data from four separate assay plates were analyzed and presented as described in Materials and Methods. A noncompetitive fit to the data is shown. The inset double-reciprocal plot shows points from 0.05 to 1 relative activity and 12.8−200 nM aggrecan for inhibitor levels 0, 15.6, 62.5, and 250 nM. Solid lines show the fit of the noncompetitive model, and dashed lines show the fit to an uncompetitive model. (b) IC_{50} values for SC81956 at the indicated concentrations of aggrecan, obtained from the data in panel a. Error bars indicate the formal standard error for each IC_{50}. The solid and dashed lines labeled Noncomp, Comp, and Uncomp indicate the expected relationship of IC_{50} to aggrecan concentration for a noncompetitive, competitive, and uncompetitive inhibitor, respectively.

from the bovine nasal cartilage assay, the full 4-parameter IC_{50} equation was modified to allow global fitting of both control (without IL-1) and SC81956 dose−response data. This was done by fitting the dose−response data to the full 4-parameter equation, $y = (\text{Range}/(1 + (x/IC_{50})^s) + \text{Min}$, and simultaneously fitting the control data to the equation $y = \text{Min}$. In these equations, y is the measured assay response, Range is the maximum y range, x is inhibitor concentration, IC_{50} is the concentration of inhibitor that gives one-half-maximal response, s is the slope factor, and Min is the minimum y. To facilitate the graphical representation of these data (Figure 2), the assay responses were expressed as % maximum relative to the fitted values for Range and Min.

For fitting aggrecanase inhibition assay data at different concentrations of aggrecan and SC81956, the standard equations for competitive, noncompetitive, and uncompetitive inhibition were modified for global fitting of assay results from four separate assay plates, allowing for independent backgrounds and V_{max} values for each plate and common values for K_m and K_i across all four plates. This was done because of small differences in incubation time with the *p*-nitrophenyl phosphate detection reagent and to increase the confidence level of the resulting fits. Comparison between the different models was made using the F test option in the GraFit software. To allow the data from all four assay plates to be shown on one graph, the data for Figure 3a are shown scaled to the range 0−1 using the background and V_{max} values for each plate. Although individual assay points were used to fit to the various models, for better clarity the data for Figure 3a are presented as means and standard deviations ($n = 8$, except 5.12 nM aggrecan and 15.6 nM SC81596 (7 observations); 80 nM aggrecan and 0 nM SC81956 (6 observations); and 200 nM aggrecan and 0 nM SC81956 (6 observations)). Additionally, these individual scaled data points were used to generate the IC_{50} values presented in Figure 3b and the comparative fits presented in Table 1. To validate the use of scaled data for these purposes, almost identical values for K_m and K_i (differing by 0.2% or less) were obtained for fits to the competitive, noncompetitive, and uncompetitive models, whether the original or scaled data points were used.

RESULTS

SC81956 Loses Significant Potency in the Bovine Nasal Cartilage Assay Compared to a Purified Enzyme Assay. The hydroxamic acid inhibitor, SC81956, was a nanomolar inhibitor of ADAMTS-4 and ADAMTS-5 when measured

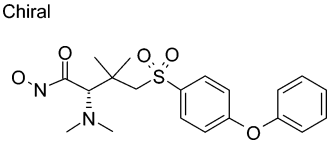

Table 1: Parameter Values (± Formal Standard Errors) That Result When the Data of Figure 3a Are Fit to Various Models

equation	$k_p[E]_t$[a]	K_S (nM)	K_i (nM)	K_{S*}	V_{max}[a,b]	K_m[c]
noncomp[d]	1.00 ± 0.03	61.1 ± 3.9	22.8 ± 1.5		1.00	61.1
eq 3	3.15E13[e]	61.1 ± 4.0	22.8 ± 1.5	3.15E13[e]	1.00	61.1
eq 3 ($K_{S*} = 10$)	11.0 ± 0.3	66.6 ± 4.3	21.4 ± 1.4	10 (fixed)	1.00	60.5

[a] Because the data in Figure 3a are scaled to the range 0−1 using the background and V_{max} values for each of four assay plates (see Materials and Methods), a composite scaling factor is included in all of the fitted values for $k_p[E]_t$. As a result, these values and the calculated values for V_{max} are dimensionless, and the values for $k_p[E]_t$ and V_{max} are 1.00 for the noncompetitive fit, [b] Equivalent to $k_p[E]_t$ for the noncompetitive model (see footnote *d*) and $k_p[E]_t/(1 + K_{S*})$ for eq 3 (see eq 4, Discussion). Note that $k_p[E]_t/(1 + K_{S*})$ approaches $k_p[E]_t/K_{S*}$ as K_{S*} becomes very large. [c] Equivalent to K_S for the noncompetitive model (see footnote *d*) and $K_SK_{S*}/(1 + K_{S*})$ for eq 3 (see eq 4, Discussion). Note that $K_SK_{S*}/(1 + K_{S*})$ approaches K_S as K_{S*} becomes very large. [d] Noncompetitive inhibition, $v = k_p[E]_t[S]/(K_S(1 + [I]/K_i) + [S](1 + [I]/K_i))$. The values for K_S and K_i differ slightly from those given in the text (61.1 ± 4.0 and 22.9 ± 1.5 nM, respectively) because for ease in presentation, the fits in this Table employ the scaled data in Figure 3a as opposed to the original data prior to scaling (see Materials and Methods). [e] These values both had formal standard errors of 5.9E18.

using purified recombinant enzyme and aggrecan substrate in the aggrecanase inhibition assay. The average IC_{50} for ADAMTS-4 was 28 nM (geometric mean for 264 measurements; geometric standard deviation range 14−59 nM), and for ADAMTS-5, the average IC_{50} was 14 nM (282 measurements, geometric standard deviation range 6−29 nM). SC81956 was also a nanomolar or subnanomolar inhibitor of matrix metalloproteinases-1, -2, -3, -8, -9, and -14 (unpublished experiments).

It has previously been shown that IL-1 induces aggrecan breakdown in bovine cartilage explant cultures and that the observed aggrecan breakdown is mediated exclusively by the aggrecanases (*17*). Therefore, the efficacy of SC81956 was tested in bovine nasal cartilage stimulated with IL-1 for 48 h in the presence or absence of compound at concentrations ranging from 3 to 3000 nM. In four separate experiments, SC81956 blocked GAG release in a concentration dependent manner with IC_{50} values of 2.0, 2.5, 2.7, and 3.3 μM (Figure 2a) and inhibited the release of neoepitope ARGS-containing fragments with IC_{50} values of 6.3, 9.3, 10.1, and 14.0 μM (Figure 2b). The average (geometric mean) IC_{50} values for GAG release (2.6 μM) and ARGS release (9.5 μM), although within 4-fold of each other, were from 93- to 678-fold higher than the IC_{50} values against either recombinant ADAMTS-4 or recombinant ADAMTS-5. This loss of potency in the bovine nasal cartilage degradation assay was observed with several other structurally related aggrecanase inhibitors (data not shown).

SC-81956 Does Not Demonstrate Competitive Inhibition of ADAMTS-4 with Respect to Aggrecan. One reason for the decreased efficacy of SC81956 in the bovine nasal cartilage assay could be the high levels of aggrecan in the cartilage matrix, which might be expected to compete with the inhibitor and reduce its potency according to the relationship given by Cheng and Prusoff for competitive inhibitors, $IC_{50} = K_i^*(1 + [S]/K_m)$ (*18*). To test this hypothesis, the aggrecan concentration dependence of ADAMTS-4 activity was determined at several concentrations of SC81956. The results (Figure 3a) were not suggestive of competition between aggrecan and SC81956. Instead, the results were described significantly better by a noncompetitive model than by a competitive model (F-test, $p < 0.02$). An uncompetitive model also fit the data but was statistically indistinguishable from the noncompetitive model (F-test, $p = 0.93$). For the noncompetitive fit to the data shown in Figure 3a, the values of kinetic constants with their formal standard errors were $K_m = 61.1 \pm 4.0$ nM and $K_i = 22.9 \pm 1.5$ nM. The corresponding values for an uncompetitive fit were $K_m = 70.7 \pm 4.9$ nM and $K_i = 14.5 \pm 1.1$ nM. The double reciprocal plot inset to Figure 3a shows the potential for these data to fit either a noncompetitive or uncompetitive model, with the overall conclusion that the points of *y*-axis intersection $1/V_{max(app)}$ vary significantly with inhibitor concentration and additionally suggest that the inhibition is not competitive. Viewing these data another way (Figure 3b), the IC_{50} for SC81956 remained essentially unchanged when the concentration of aggrecan was raised to a value that was over 3 times its apparent K_m. If aggrecan competed with SC81956, the relationship of Cheng and Prusoff (*18*) would have predicted an increase of about 3.5-fold in the IC_{50} as aggrecan increased from 12.8 to 200 nM or from 0.2 to 3.3 times the apparent K_m (Figure 3b). Alternatively, the relationship of Cheng and Prusoff for uncompetitive inhibitors, $IC_{50} = K_i^*(1 + K_m/[S])$ (*18*), suggests that the IC_{50} should increase dramatically at low concentrations of aggrecan, achieving a value of 94 nM at 12.8 nM aggrecan (0.2 times the apparent K_m) (Figure 3b). Because the IC_{50} values fail to show an increase at aggrecan concentrations significantly above or below the K_m, this suggests that the inhibition data are better described by the noncompetitive model where the IC_{50} is predicted to be invariant with substrate concentration (*18*).

SC81956 Is Competitive with a Low Molecular Weight Peptide Substrate of ADAMTS-4. Attempts to demonstrate direct competition between SC81956 and most low molecular weight peptide substrates of ADAMTS-4 were problematic because in each case the substrate K_m appeared to be above its solubility limit, and saturation could not be reliably demonstrated. One such peptide substrate is Peptide-B06, a novel fluorogenic peptide substrate (see Materials and Methods). However, competition between SC81956 and a more soluble non-fluorogenic peptide substrate, Peptide-A08, was readily demonstrated. Peptide-A08 had an effective IC_{50} of 26 μM when fluorogenic Peptide-B06 was used as substrate. Increasing levels of Peptide-A08 from 0 to 100 μM increased the apparent IC_{50} of SC81956 in a manner expected for two mutually exclusive inhibitors (Figure 4). A direct fit of the velocity data of Figure 4a as a function of both Peptide-A08 and SC81956 concentrations using eq 2 (see Materials and Methods) yielded the same conclusion. The predicted mutually exclusive effect of Peptide-A08 on the IC_{50} of SC81956 on the basis of this fit is shown in Figure 4b and is similar to the observed IC_{50} values. These results suggest that SC81956 is competitive with Peptide-A08, a small peptide substrate of ADAMTS-4.

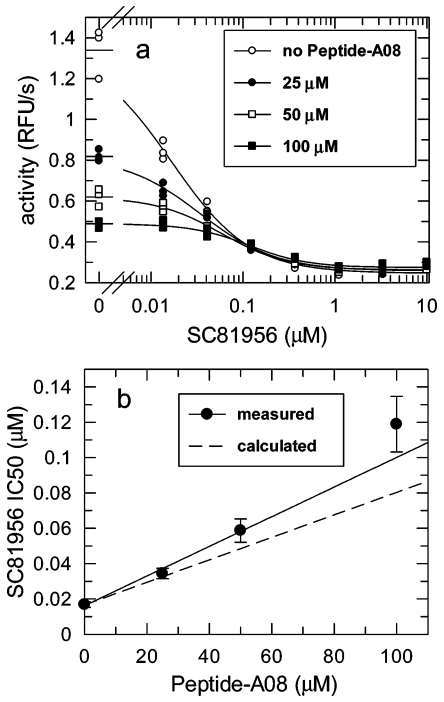

FIGURE 4: SC81956 interacts in a mutually exclusive fashion with a low molecular weight peptide substrate of ADAMTS-4. (a) Results from the fluorescent peptide substrate assay conducted in the presence of cleavable nonfluorescent Peptide-A08 and SC81956 as described in Materials and Methods. Solid curves show the best fits of these data to the four parameter equation for IC_{50} determinations. (b) IC_{50} values from the data in panel a plotted versus Peptide-A08 concentration. The solid line (measured) indicates a linear regression weighted according to the formal standard errors. The dashed line (calculated) indicates the relationship of IC_{50} to Peptide-A08 concentration that would be expected from the fit of the data in panel a to eq 2, describing a mutually exclusive interaction between SC81956 and Peptide-A08.

Theoretical Model Predicts that Active-Site Inhibitors Could Appear Noncompetitive versus the Native Aggrecan Substrate. As described in the introduction and summarized in Figure 1, the concentration of aggrecan for half-maximal binding of ADAMTS-4 has been reported to be about 11 nM and appears to be mediated by an interaction between the thrombospondin domain of ADAMTS-4 and the many GAG chains of aggrecan (*5*). This compares with the 61 nM K_m for ADAMTS-4 mediated cleavage of aggrecan determined experimentally (Figure 3a). In contrast, the K_m for ADAMTS-4 cleavage of an optimal peptide derived from the Glu^{373} cleavage site in aggrecan has been reported to be 480 μM (*8*), and in this study, we have shown that the substrate Peptide-A08 has an IC_{50} of 26 μM, suggesting a K_m of the same magnitude. Enzymatic deglycosylation of native aggrecan dramatically reduces its cleavage by aggrecanase, as does the addition of free glycosaminoglycans (*5*, *19*). Combined with the observation that an active site inhibitor appears to be noncompetitive, these data suggest the rapid equilibrium model for aggrecan cleavage by aggrecanase diagrammed in Scheme 1.

In this model, aggrecan (S) binds to aggrecanase (E) in two steps: initial binding at an exosite to form ES, followed by the formation of the Michaelis complex with the appropriate peptide sequence at the active site (ES*). This is presented as an ordered process because the large difference in peptide K_m and aggrecan K_d for the interaction of substrates with aggrecanase suggests that exosite binding occurs first. In addition, initial binding of aggrecan at the active site is not expected based on the lack of competition observed between SC81956 and aggrecan. A key feature of the model in Scheme 1 is that an inhibitor (I) competitive with peptide substrate such as SC81956 binds both free enzyme and the initial aggrecan−aggrecanase exosite complex but is excluded by the subsequent Michaelis complex. ES and ES* are in equilibrium as described by the dissociation constant K_{S*}. It should be pointed out that Scheme 1 is only intended to describe the interaction of the native aggrecan substrate with aggrecanase. Small peptide substrates that lack the exosite interaction should bind directly to the active site and show competition with inhibitors as described by simple inhibition models (*20*).

The initial rate equation based on this model (eq 1 with $\alpha = 1$; see Materials and Methods) can be written as follows:

$$v = (k_p[E]_t/K_{S*})[S]/(K_S(1 + [I]/K_i) + [S](1 + 1/K_{S*} + [I]/K_i)) \quad (3)$$

Examination of eq 3 reveals that as K_{S*} becomes large ($\gg$1), eq 3 reduces to the same form as that of the general rate equation describing noncompetitive inhibition (where $k_p[E]_t/K_{S*}$ approaches V_{max}, and K_S approaches the Michaelis constant, K_m) because the $1/K_{S*}$ term in the denominator becomes insignificant. If K_{S*} is large, the enzyme−substrate complex is predominantly in a form (ES) that can still bind inhibitor regardless of the level of substrate, giving rise to apparent noncompetitive inhibition. Fitting eq 3 to the data of Figure 3a results in a seemingly identical fit to the data where both $k_p[E]_t$ and K_{S*} become extremely large ($\sim$1E13) with even larger formal standard errors (Table 1), suggesting that these data are not sufficient to determine the values of either k_p or K_{S*}. In comparison to the noncompetitive fit parameters determined for Figure 3a (Table 1), the ratio $k_p[E]_t/K_{S*}$ from the fit to eq 3 was numerically the same as the noncompetitive V_{max}, the K_i values were the same, and K_S was numerically equal to the K_m determined from the noncompetitive fit. Although it was not possible to determine the actual magnitude of K_{S*} from these data, it should be noted that fixing K_{S*} at the relatively modest value of 10 resulted in a fit to eq 3 that appeared very similar to that shown in Figure 3a, and values for $k_p[E]_t$, K_S, and K_i yielded calculations of V_{max} and K_m that were also very similar to those obtained from the unconstrained fit to eq 3 (Table 1). Using these values, it can be calculated that under the condition $K_{S*} = 10$, the IC_{50} for SC81956 would remain essentially unchanged (21.7−23.0 nM over the range 12.8−200 nM aggrecan), similar to that observed in Figure 3b. Observations consistent with a value for K_{S*} that is significantly greater than 1 will be presented below.

Although the two-step model of substrate binding in Scheme 1 represents a simplification of what is known about the cleavage of aggrecan by aggrecanase, there is reason to believe that it is still adequate in describing the system. First, while there are multiple cleavage sites and products resulting from the aggrecanase reaction, it has been observed that the appearance of the ^{374}ARGS neoepitope is linear with time during the 6 h incubation period in the aggrecanase inhibition assay described above. This implies that although other sites of cleavage may be preferred, there is no obligatory order,

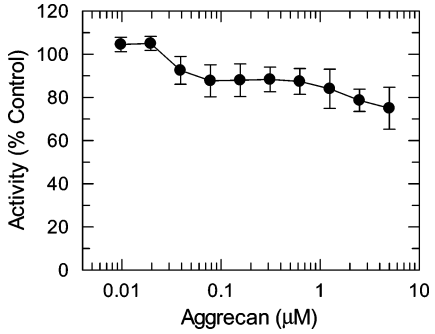

FIGURE 5: Increasing levels of aggrecan have little effect on the cleavage of a low molecular weight peptide substrate by ADAMTS-4. Rates of Peptide-B06 cleavage are expressed as a percentage of the rate in the absence of aggrecan. Shown is the average of three replicates with standard deviations indicated as error bars.

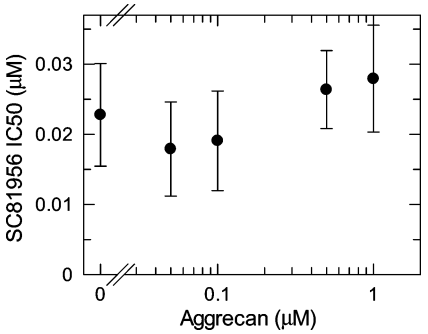

FIGURE 6: Increasing levels of aggrecan have no effect on the potency of SC81956 inhibition of ADAMTS-4 measured using a low molecular weight peptide substrate. The potency of SC81956 inhibition (IC_{50}) in the fluorescent peptide substrate assay was determined as described in Materials and Methods. Error bars indicate the formal standard errors associated with the IC_{50} fit.

and each cleavage can be treated independently. Second, while the model suggests a single site for the exosite-mediated binding of aggrecan and aggrecanase, there are certainly many such sites because of the multiple sulfated GAG chains present on the substrate. Thus, the K_S in this model certainly represents an overall dissociation constant resulting from a large number of interactions. However, as long as each of these interactions does not exclude inhibitor from binding at the active site of the enzyme, they can be treated as a single interaction for purposes of the model. The key feature of the model is that the enzyme−substrate complex is initially in a form where inhibitor is free to bind to the enzyme which is then followed by the formation of an inhibitor-excluding Michaelis complex. This could be accomplished by a single higher affinity interaction that subsequently undergoes a conformational change to form the Michaelis complex or via a large number of weaker interactions that allow the enzyme to probe the substrate for the appropriate cleavage site. Finally, it should be noted that because the ^{374}ARGS neoepitope measured by the assay used in this study represents the least preferred of the five sites cleaved by the enzyme, the substrate is not a single entity but a constantly changing mixture of increasingly processed aggrecan species (*3*). This could significantly complicate the kinetics of the ^{374}ARGS cleavage reaction if either exosite binding (K_S) or the subsequent transition to Michaelis complex (K_{S*}) are influenced by these other cleavages. Implicit in acceptance of this model is that such cleavages do not significantly affect these fundamental interactions, a possibility supported by the observed linear reaction kinetics mentioned above.

Hydrolysis of a Low Molecular Weight Peptide Substrate and Inhibition by SC81956 Is Unaffected by High Levels of Aggrecan. The model in Scheme 1 predicts apparent noncompetitive inhibition if K_{S*} is large. If K_{S*} is large, the predominant form of the enzyme−substrate complex might allow the binding and cleavage of a low molecular weight substrate. Accordingly, increasing amounts of aggrecan were shown to cause only a small decrease in the hydrolysis rate of Peptide-B06, the fluorogenic peptide substrate of ADAMTS-4 (Figure 5). This supports the prediction that binding of aggrecan to ADAMTS-4 leaves the majority of the enzyme in a form where the active site is accessible. Additional evidence that the active site of ADAMTS-4 can be occupied by small inhibitors in the presence of high levels of aggrecan is provided by the data shown in Figure 6. Here, the potency of SC81956 inhibition of ADAMTS-4 is measured using the same Peptide-B06 substrate and is unaffected by levels of aggrecan up to 1 μM. This suggests that aggrecan and SC-81956 can bind to the enzyme in a non-exclusive manner and supports the hypothesis that the dissociation constant, K_{S*}, is relatively large. In turn, this is consistent with the observation of apparent noncompetitive inhibition made in the aggrecanase inhibition assay (Figure 3).

DISCUSSION

Substrate interactions at exosites, that is, sites removed from the active site within the enzyme−substrate complex, have been documented for ADAMTS-4. This may represent a major mechanism through which distinctive protein substrate specificities are achieved by members of the ADAMTS family of metalloproteinases. Exosite-dependent substrate recognition implies that binding interactions on areas of the enzyme distinct from the residues directly involved in catalysis contribute to substrate affinity. The data presented herein explores a consequence of the differences between the mechanism(s) underlying the recognition of a peptide substrate versus native aggrecan. Comparing the K_m reported in this study for native aggrecan cleavage by ADAMTS-4 (61 nM) with the reported K_d for the binding of aggrecan to ADAMTS-4 (11 nM) (*5*), the reported K_m for cleavage of a 41-amino acid peptide that brackets the Glu^{373} cleavage site in aggrecan (480 μM) (*8*) and the value of 26 μM obtained from the apparent IC_{50} for substrate Peptide-A08 in this study, it is clear that the K_m for aggrecan cleavage is much closer to the binding K_d than to the peptide K_m values that have thus far been reported. Thus, the K_m for the peptide substrate appears to reflect a much weaker interaction at the active site of ADAMTS-4 than is observed with aggrecan, while the much lower K_m seen with aggrecan appears to arise additionally from interactions with the TS exosite and, potentially, other exosites in the spacer domain (*21*). Examining the model in Scheme 1 and rearranging eq 1 when [I] = 0, one obtains eq 4.

$$v = k_p[E]_t[S]/(1 + K_{S*})/(K_S K_{S*}/(1 + K_{S*}) + [S]) \quad (4)$$

This expression is in the form $v = V_{max}[S]/(K_m+[S])$, with $V_{max} = k_p[E]_t/(1 + K_{S*})$ and $K_m = K_S K_{S*}/(1 + K_{S*})$. Thus, for such a two-step mode of substrate−enzyme interaction,

if $K_{S*} \gg 1$, then the observed K_m will approximate K_S, which appears to be the case for the aggrecan−ADAMTS-4 interaction.

Models similar to that outlined in Scheme 1 and eq 1 have been used by others to describe the inhibition of prothombinase (*15*, *22*), extrinsic Xase complex (*23*), and Factor XIa (*24*). In each case, recognition of the macromolecular substrate is facilitated by an initial exosite interaction, followed by the formation of the Michaelis complex, ES*. As observed in the present study, these earlier studies show that when an inhibitor that is competitive versus a small peptide substrate appears to be noncompetitive versus the native macromolecular substrate, the equilibrium between ES and ES* is significantly in favor of ES. In addition, two-step models of exosite-mediated substrate binding similar to that given here have also been proposed to explain aspects of the substrate recognition and phosphorylation kinetics of ERK2 (*25*) and PDK1 (*26*).

The present study is the first to our knowledge to employ the two-step model of exosite-mediated substrate binding described above to explain the inhibition kinetics of an enzyme acting on a non-proenzyme substrate. In addition, it is the first to report a K_m for aggrecan cleavage by aggrecanase and to examine its inhibition kinetics. The data suggest that the K_m for aggrecan cleavage by ADAMTS-4 is strongly influenced by an exosite interaction. A consequence is that inhibition that is expected to be competitive instead appears noncompetitive. The relationship of Cheng and Prusoff ($IC_{50} = K_i*(1 + [S]/K_m)$) (*18*) describes the effect of substrate competition on the observed potency of a competitive inhibitor. Proper use of this equation requires that the interactions among substrate, enzyme, and inhibitor be described by the competitive inhibition model, where inhibitor and substrate compete for the same site and cannot bind to the enzyme at the same time. Additionally, calculation of the K_i from an IC_{50} for a competitive inhibitor requires accurate knowledge of the K_m of the enzyme for the competitive substrate. The present results show that inhibition mechanisms determined with an artificial peptide substrate may not correctly describe the mechanism of inhibition when the native substrate is used. While inhibitor SC81956 appears to be competitive versus a peptide substrate, assuming this for the aggrecan substrate would lead to an incorrect application of the Cheng−Prusoff equation. IC_{50} values determined at high aggrecan concentrations would give K_i values that are numerically too small, overestimating potency. This would additionally result in incorrect estimates of relative potency between different proteases important for inhibitor selectivity and safety.

SC81956, which has a potency (IC_{50}) of 28 nM against recombinant ADAMTS-4 is 93 (GAG release)- to 339 (ARGS neoepitope)-fold less active in blocking cytokine-stimulated aggrecanase-mediated aggrecan breakdown in bovine nasal cartilage. This decreased potency has been seen with other aggrecanase inhibitors that have been tested in this assay and was previously thought to be due to the high concentration of aggrecan present in nasal cartilage (>10 mg/mL, ~10 μM). However, the present work fails to demonstrate competition between the hydroxamate compound SC81956 and aggrecan and suggests that the high concentrations of aggrecan do not explain the observed decrease in potency. Understanding what factors cause this decreased potency will be important for developing aggrecanase inhibitors for the treatment of arthritis. These factors may include general protein binding of the inhibitor, unfavorable localization of the inhibitor, or stability of the compound in the assay matrix.

The two-step model of exosite-mediated substrate binding and the observed noncompetitive behavior versus native aggrecan shown by a competitive inhibitor of ADAMTS-4 have potential implications in the identification of efficacious drugs that target this enzyme. As has been suggested by others, a reversible inhibitor that binds at the active site may have difficulties preventing the formation of the Michaelis complex from the initial enzyme−substrate exosite complex because this could be viewed as interfering with an intramolecular binding event (*10*, *15*, *23*). This implies that inhibitors that prevent the initial exosite-mediated binding could be more successful. Alternatively, the potential impact on the efficacy of active site directed inhibitors by the observed lack of competition with exosite-bound native substrate should also be considered. Competitive enzyme inhibitors can have diminished efficacy *in vivo* due to high levels of endogenous substrate, which may be further elevated because of inhibition. Successful substrate-competitive drugs are found to have additional mechanistic characteristics, such as slow off-rates or irreversibility, which overcome the effects of high endogenous substrate (*27*, *28*). The two-step mode of substrate binding exemplified by aggrecan and aggrecanase suggests another mechanism, dependent wholly on the nature of the enzyme and substrate interaction, whereby competitive inhibitors may yet be successful as drugs. Given these conflicting considerations regarding the utility of competitive inhibitors, additional work will be required to determine to what extent they might be successful as drugs in the inhibition of aggrecanase.

REFERENCES

1. Tortorella, M. D., Burn, T. C., Pratta, M. C., Abbaszade, I., Hollis, J. M., Liu, R., Rosenfeld, S. A., Copeland, R. A., Decicco, C. P., Wynn, R., et al. (1999) Purification and cloning of aggrecanase-1: a member of the ADAMTS family of proteins, *Science 284*, 1664−1666.
2. Porter, S., Clark, I., Kevorkian, L., and Edwards, D. (2005) The ADAMTS metalloproteinases, *Biochem. J. 386*, 15−27.
3. Tortorella, M. D., Pratta, M., Liu, R. Q., Austin, J., Ross, O. H., Abbaszade, I., Burn, T., and Arner, E. (2000) Sites of aggrecan cleavage by recombinant human aggrecanase-1 (ADAMTS-4), *J. Biol. Chem. 275*, 18566−18573.
4. Hardingham, T. E., Fosang, A. J., and Dudhia, J. (1992) Aggrecan, the Chondroitin Sulfate/Keratan Sulfate Proteoglycan from Cartilage, in *Articular Cartilage and Osteoarthritis* (Kuettner, K. E., Schleyerbach, R., Peyton, J. G., and Hascall, V. C., Eds.) pp 5−20, Raven Press, New York.
5. Tortorella, M., Pratta, M., Liu, R. Q., Abbaszade, I., Ross, H., Burn, T., and Arner, E. (2000) The thrombospondin motif of aggrecanase-1 (ADAMTS-4) is critical for aggrecan substrate recognition and cleavage, *J. Biol. Chem. 275*, 25791−25797.
6. Yao, W., Wasserman, Z. K., Chao, M., Reddy, G., Shi, E., Liu, R. Q., Covington, M. B., Arner, E. C., Pratta, M. A., Tortorella, M., et al. (2001) Design and synthesis of a series of (2r)-n(4)-hydroxy-2-(3-hydroxybenzyl)-n(1)-[(1s,2r)-2-hydroxy-2,3-dihydro-1h-inden-1ryl]butanediamide derivatives as potent, selective, and orally available aggrecanase inhibitors, *J. Med. Chem. 21*, 3347−3350.
7. Cherney, R., Mo, R., Meyer, D., Wang, L., Yao, W., Wasserman, Z., Liu, R., Covington, M., Tortorella, M., Arner, E., et al. (2003) Potent and selective aggrecanase inhibitors containing cyclic P1 substituents, *Bioorg. Med. Chem. Lett. 13*, 1297−1300.

8. Miller, J., Liu, R., Davis, G., Pratta, M., Trzaskos, J., and Copeland, R. (2003) A microplate assay specific for the enzyme aggrecanase, *Anal. Biochem. 314*, 260−265.
9. Zhang, Y., Xu, J., Levin, J., Hegen, M., Li, G., Robertshaw, H., Brennan, F., Cummons, T., Clarke, D., Vansell, N., et al. (2004) Identification and Characterization of 4-[[4-(2-butynyloxy)phenyl]sulfonyl]-N-hydroxy-2,2-dimethyl-(3S)thiomorpholinecarboxamide (TMI-1), a novel dual tumor necrosis factor−converting enzyme/matrix metalloprotease inhibitor for the treatment of rheumatoid arthritis, *J. Pharmacol. Exp. Ther. Fast Forward 309*, 348−355.
10. Krishnaswamy, S. (2005) Exosite-driven substrate specificity and function in coagulation, *J. Thromb. Haemostasis 3*, 54−67.
11. Hughes, C. E., Caterson, B., Fosang, A. J., Roughley, P. J., and Mort, J. S. (1995) Monoclonal antibodies that specifically recognize neoepitope sequences generated by 'aggrecanase' and matrix metalloproteinase cleavage of aggrecan: application to catabolism in situ and in vitro, *Biochem. J. 305*, 799−804.
12. Farndale, R. W., Buttle, D. J., and Barrett, A. J. (1986) Improved quantitation and discrimination of sulphated glycosaminoglycans by use of dimethylmethylene blue, *Biochim. Biophys. Acta 883*, 173−177.
13. Hills, R., Mazzarella, R., Fok, K., Liu, M., Nemirovsky, O., Leone, J., Zack, M. D., Arner, E. C., Viswanathan, M., Abujoub, A., Muruganandam, A., Sexton, D. J., Bassill, G. J., Sato, A. K., Malfait, A.-M., and Tortorella, M. D. (2007) Identification of an ADAMTS-4 cleavage motif using phage display leads to the development of fluorogenic peptide substrates and reveals matrilin-3 as a novel substrate, *J. Biol. Chem. 282*, 11101−11109.
14. Segal, I. H. (1993) *Enzyme Kinetics, Behavior and Analysis of Rapid Equilibrium and Steady-State Enzyme Systems*, Wiley Classics Library Edition, pp 22−24, John Wiley & Sons, Inc., New York.
15. Krishnaswamy, S., and Betz, A. (1997) Exosites determine macromolecular substrate recognition by prothrombinase, *Biochemistry 36*, 12080−12086.
16. Copeland, R. A. (2000) *Enzymes, A Practical Introduction to Structure, Mechanism, and Data Analysis*, 2nd ed., pp 288−289, John Wiley & Sons, Inc., New York.
17. Tortorella, M. D., Malfait, A. M., Decicco, C., and Arner, E. (2001) The role of ADAM-TS4 (aggrecanase-1) and ADAM-TS5 (aggrecanase-2) in a model of cartilage degradation, *Osteoarthritis and Cartilage 9*, 539−552.
18. Cheng, Y.-C., and Prusoff, W. H. (1973) Relationship between the inhibition constant (K_I) and the concentration of inhibitor which causes 50 per cent inhibition (I_{50}) of an enzymatic reaction, *Biochem. Pharmacol. 22*, 3099−3108.
19. Sugimoto, K., Takahashi, M., Yamamoto, Y., Shimada, K., and Tanzawa, K. (1999) Identification of aggrecanase activity in medium of cartilage culture, *J. Biochem. 126*, 449−455.
20. Segal, I. H. (1993) *Enzyme Kinetics, Behavior and Analysis of Rapid Equilibrium and Steady-State Enzyme Systems*, Wiley Classics Library Edition, pp. 100−123, John Wiley & Sons, Inc., New York.
21. Zeng, W., Corcoran, C., Collins-Racie, L. A., Lavallie, E. R., Morris, E. A., and Flannery, C. R. (2006) Glycosaminoglycan-binding properties and aggrecanase activities of truncated ADAMTSs: comparative analysis with ADAMTS-5, -9, -6 and -18, *Biochem. Biophys. Acta 1760*, 517−524.
22. Boskovic, D. S., and Krishnaswamy, S. (2000) Exosite binding tethers the macromolecular substrate to the prothrombinase complex and directs cleavage at two spatially distinct sites, *J. Biol. Chem. 275*, 38561−38570.
23. Baugh, R. J., Dickinson, C. D., Ruf, W., and Krishnaswamy, S. (2000) Exosite interactions determine the affinity of factor X for the extrinsic Xase complex, *J. Biol. Chem. 275*, 28826−28833.
24. Ogawa, T., Verhamme, I. M., Sun, M. F., Bock, P. E., and Gailani, D. (2005) Exosite-mediated substrate recognition of factor IX by factor XIa. The factor XIa heavy chain is required for initial recognition of factor IX, *J. Biol. Chem. 280*, 23523−23530.
25. Rainey, M. A., Callaway, K., Barnes, R., Wilson, B., and Dalby, K. N. (2005) Proximity-induced catalysis by the protein kinase ERK2, *J. Am. Chem. Soc. 127*, 10494−10495.
26. Gao, X., and Harris, T. K. (2006) Steady-state kinetic mechanism of PDK1, *J. Biol. Chem. 281*, 21670−21681.
27. Swinney, D. C. (2004) Biochemical mechanisms of drug action: what does it take for success?, *Nat. Rev. Drug Discovery 3*, 801−808.
28. Robertson, J. G. (2005) Mechanistic basis of enzyme-targeted drugs, *Biochemistry 44*, 5561−5571.

BI7000642